Available online at www.sciencedirect.com
SCIENCE DIRECT®
Materials Chemistry and Physics 80 (2003) 309–318
MATERIALS CHEMISTRY AND PHYSICS
www.elsevier.com/locate/matchemphys

Solid-state synthesis and electrochemical characterization of $LiM_yCr_{0.5-y}Mn_{1.5}O_4$ (M = Fe or Al; 0.0 < y < 0.4) spinels

George Ting-Kuo Fey*, Cheng-Zhang Lu, T. Prem Kumar[1]

Department of Chemical and Materials Engineering, National Central University, Chung-Li 32054, Taiwan, ROC

Received 31 July 2002; received in revised form 11 October 2002; accepted 17 October 2002

Abstract

A series of $LiM_yCr_{0.5-y}Mn_{1.5}O_4$ compositions, where M is either Fe or Al, was synthesized by a conventional solid-state fusion method. Phase-pure materials were obtained for all the Fe-substituted compositions, while at Al stoichiometries of 0.3 and 0.4 the Al-substituted compositions had γ–$LiAlO_2$ as an impurity phase. An increase in the amount of Fe or Al increased the lattice parameters as well as the propensity of these co-dopants to occupy the 8*a* lithium sites. Electrochemical activity was noted in the 4 and 5-V regions. Fe as a co-substituent increased the currents associated with the high-voltage peaks, while Al as a co-substituent enhanced the high-voltage capability of the spinel. Irrespective of whether the co-substituent was a transition metal or non-transition metal, it altered the electrochemical characteristics of both the Mn^{4+}/Mn^{3+} and the Cr^{4+}/Cr^{3+} couples, the effect being more pronounced in the 5-V region. Although increased amounts of Fe or Al rendered the spinels high-voltage active, both the deliverable capacity and capacity retention were lowered. The cumulative capacity obtained with Al-substituted materials was less than with Fe-substituted materials. At a 0.1 C rate between 3.3 and 5.1 V, the Fe co-substituted spinel ($y = 0.1$) gave a first-cycle capacity of 117 mAh g^{-1}, while that with Al was 112 mAh g^{-1}. The corresponding values in the 40th cycle were 88 and 82 mAh g^{-1}.

Keywords: $LiMn_2O_4$; Substituted $LiMn_2O_4$; Oxide cathodes; Lithium intercalation; Lithium-ion battery

1. Introduction

$LiMn_2O_4$ has a cubic structure of *Fd*3*m* symmetry in which the Li^+ and the Mn^{3+}/Mn^{4+} are located in the 8*a* tetrahedral and 16*d* octahedral sites, respectively, in a cubic closely packed array of O^{2-} ions, which occupy the 32*e* sites [1,2]. The 8*a* sites share a face with the vacant 16*c* octahedral sites, providing three-dimensional channels for the reversible intercalation of lithium ions. Lithium extraction from the 8*a* sites occurs at 4.1 V versus Li^+/Li, yielding λ-MnO_2 upon complete lithium extraction. The cyclability of this cathode is related to the structural integrity of the host lattice during the charge–discharge processes [3]. Although the charge–discharge processes in the 4-V region are accompanied by a 7.6% volume change in the unit cell, the change is so gradual and isotropic that the cubic symmetry of the material is usually maintained [4]. However, prolonged cycling, especially at elevated temperatures, results in a capacity fade [5–7]. Attempts have been made to improve the cyclability of the spinel in the 4-V region by partially substituting manganese with transition metals like chromium, cobalt, iron, nickel, titanium and zinc, and non-transition metals such as aluminum, gallium, germanium and magnesium. Substituting part of the manganese with another metal may increase the stability of the spinel structure [8,9] or may raise the operating voltage of the system [10], often at the expense of the deliverable capacity [8–10]. Although such substitutions often result in enhanced stability of the spinel, the first discharge capacity is found to be considerably lower than the parent compound. The reduction in capacity is due to the fact that the substituent ions do not get oxidized or reduced in the 4-V region. According to Sigala et al. [11] and Zhang et al. [12], the capacity loss in the 4-V region for $LiM_yMn_{1-y}O_4$, where M is a transition metal ion like chromium or nickel, reappears at a higher voltage (4.7 V for nickel and 4.9 V for chromium), which gives their discharges a two-step profile. Therefore, charging of such systems must be done at voltages above 5-V.

Cr^{3+} as a substituent has been investigated by a number of groups [8,13–20]. Chromium has been shown to form

* Corresponding author. Tel.: +886-3-425-7325/422-7151x4206; fax: +886-3-425-7325.
E-mail address: gfey@cc.ncu.edu.tw (G.T.-K. Fey).
[1] On deputation from: Central Electrochemical Research Institute, Karaikudi 630006, TN, India.

0254-0584/02/$ – see front matter © 2002 Elsevier Science B.V. All rights reserved.
PII: S0254-0584(02)00522-9

solid solutions of the form $LiCr_yMn_{2-y}O_4$ [13]. With an increase in chromium content, the 4-V capacity decreases, but additional capacity may be tapped at about 4.9 V [8,11,21]. The higher stabilization energy of Cr^{3+} for octahedral coordinations is well known [22]. Chromium incorporation has been shown to stabilize the spinel structure by enhancing Mn–O covalency, removing manganese from the tetrahedral sites, and reducing the Jahn–Teller effect [17]. Similarly, Fe^{3+} has also been investigated as a substituent in $LiMn_2O_4$ [23–25]. Substitution with iron is believed to result in a disordered structure, which lessens the Jahn–Teller distortion, resulting in better cyclability of the spinel in the 3-V region [23]. Song et al. [24] reported that iron decreased the 4-V capacity, but improved the cycling performance. Ohzuku et al. [25] reported the formation of a series of solid solutions of the general formula $LiFe_yMn_{1-y}O_4$ and discussed the electrochemical lithium intercalation in these materials based on the results of their Mossbauer spectroscopic studies. Aluminum as a non-transition metal substituent reduces strain in $LiMn_2O_4$ during repeated cycling [26,27], and facilitates a higher discharge capacity retention [27]. However, Lee et al. [28] observed a unique effect with aluminum-substituted $LiMn_2O_4$ prepared by a melt-impregnation method: while the substituent led to excellent cycling performance in the 4-V region, it produced an abrupt capacity loss in the 3-V region. The authors [28] attributed this effect to the formation of mixed cubic and tetragonal phases after some initial cycling.

In this paper, we report the results of our study on the effect of co-substituting $LiCr_{0.5}Mn_{1.5}O_4$ with iron or aluminum. While the stoichiometry of the manganese was maintained at the molar ratio of 1.5, the chromium was partially substituted with iron or aluminum. The molar ratios of the co-substituents were 0.0, 0.1, 0.2, 0.3 and 0.4. Their effects on the structural and electrochemical properties of the spinel are discussed and correlations are drawn.

2. Experimental

The substituted compounds, $LiM_yCr_{0.5-y}MnO_4$ (M = Fe or Al; y = 0.0, 0.1, 0.2, 0.3 and 0.4), were synthesized by a solid-state fusion method from oxide, carbonate and hydroxide precursors. Stoichiometric amounts of Li_2CO_3 (Ferax), MnO_2 (Aldrich) and Cr_2O_3 (Merck) and the desired substituent compound, Fe_2O_3 (Ferax) or $Al(OH)_3$ (J.T. Baker), were thoroughly ground in an agate mortar and pelletized. The pellets were then fired in a muffle furnace at 800 °C for 24 h in air. The heating rate was 4.2 °C min^{-1} and the cooling rate to room temperature was 3 °C min^{-1}. After cooling to room temperature, the pellets were ground again. The chemical compositions of the products were analyzed by an inductively coupled plasma-mass spectrometer (PE-Sciex Elan Model 6100 DRC). They are listed in Table 1and were found to be close to the targeted formulae. The changes in the local structure of the parent compound as a result of the substitution were studied by a Siemens D5000 X-ray diffractometer with nickel-filtered Cu Kα radiation between scattering angles 5 and 80° in increments of 0.05°.

Charge–discharge studies were carried out with coin cells assembled in standard 2032 cell hardware. Lithium metal was used as the anode and a 1 M solution of $LiPF_6$ in EC:DEC (1:1 v/v) (Tomiyama Chemicals) was used as the electrolyte. The cathode was prepared by blade-coating a slurry of 85 wt.% active material with 10 wt.% conductive carbon black and 5 wt.% poly(vinylidene fluoride) binder in *N*-methyl-2-pyrrolidone on an aluminum foil, drying overnight at 120 °C in an oven, roller-pressing the dried coated foil, and punching out circular discs. Cell assembly was done in an argon-filled glove box (VAC, MO 40-1) that contained less than 2 ppm oxygen and moisture. The cells were cycled at a 0.1C rate between 3.3 and 5.2 V in a multi-channel battery tester (Maccor 4000).

A slow scan cyclic voltammetric (SSCV) experiment was performed in a three-electrode glass cell placed inside the glove box. The working electrodes were prepared with the cathode powders as described above, but coated on both sides of the aluminum foil. The cells for SSCV studies were assembled inside the glove box with lithium metal foil serving as both counter and reference electrodes. The electrolyte used was the same as the one used for the coin cell. Cyclic voltammograms were run on a Solartron 1287 Electrochemical Interface at a scan rate of 0.1 mV s^{-1} between 3.0 and 5.1 V.

Table 1
ICP-MS and XRD data for $LiM_yCr_{0.5-y}Mn_{1.5}O_4$ (M = Fe or Al; y = 0.0, 0.1, 0.2, 0.3 and 0.4)

Composition	ICP-MS analysis	a (Å)	$I_{(400)}/I_{(311)}$	$I_{(220)}/I_{(311)}$	Unit Cell Volume (Å)^3
$LiMn_2O_4$	$Li_{0.970}Mn_{1.982}O_{3.977}$	8.2000	1.036	*	551
$LiCr_{0.5}Mn_{1.5}O_4$	$Li_{0.973}Cr_{0.478}Mn_{1.489}O_{3.951}$	8.1528	1.069	*	542
$LiFe_{0.1}Cr_{0.4}Mn_{1.5}O_4$	$Li_{0.984}Cr_{0.386}Fe_{0.098}Mn_{1.483}O_{3.933}$	8.1616	1.038	*	544
$LiFe_{0.2}Cr_{0.3}Mn_{1.5}O_4$	$Li_{0.954}Cr_{0.299}Fe_{0.196}Mn_{1.430}O_{3.810}$	8.1932	1.027	*	550
$LiFe_{0.3}Cr_{0.2}Mn_{1.5}O_4$	$Li_{0.948}Cr_{0.183}Fe_{0.305}Mn_{1.450}O_{3.840}$	8.1968	1.010	0.037	551
$LiFe_{0.4}Cr_{0.1}Mn_{1.5}O_4$	$Li_{0.943}Cr_{0.104}Fe_{0.410}Mn_{1.462}O_{3.903}$	8.2144	0.964	0.042	554
$LiAl_{0.1}Cr_{0.4}Mn_{1.5}O_4$	$Li_{0.984}Cr_{0.391}Al_{0.095}Mn_{1.485}O_{3.943}$	8.1616	1.071	*	543
$LiAl_{0.2}Cr_{0.3}Mn_{1.5}O_4$	$Li_{0.972}Cr_{0.294}Al_{0.188}Mn_{1.479}O_{3.921}$	8.1720	1.035	*	546
$LiAl_{0.3}Cr_{0.2}Mn_{1.5}O_4$	$Li_{0.968}Cr_{0.191}Al_{0.293}Mn_{1.482}O_{3.927}$	8.1832	0.980	*	548
$LiAl_{0.4}Cr_{0.1}Mn_{1.5}O_4$	$Li_{0.952}Cr_{0.101}Al_{0.398}Mn_{1.467}O_{3.942}$	8.1932	0.920	*	550

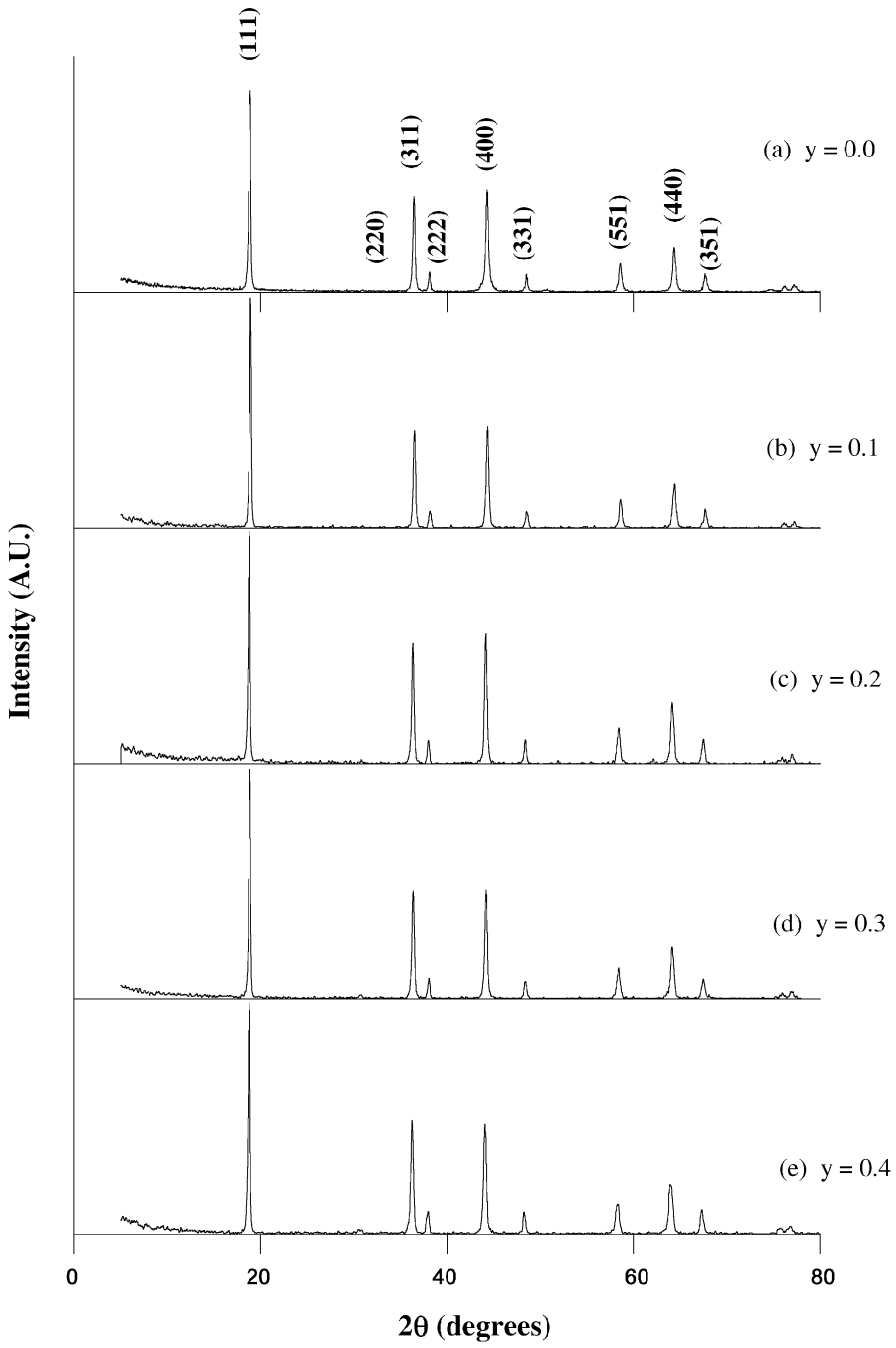

Fig. 1. Powder X-ray diffraction patterns of the $LiFe_yCr_{0.5-y}Mn_{1.5}O_4$ compositions.

3. Results and discussion

3.1. X-ray diffraction

Typical powder X-ray diffraction patterns recorded for the Fe- and Al-substituted $LiCr_{0.5}Mn_{1.5}O_4$ compositions are shown in Figs. 1 and 2, respectively. All the Fe-substituted compositions were found to be phase-pure, with all the peaks indexable in the *Fd*3*m* space group with a cubic lattice. However, with the Al-substituted compositions a few extra peaks could be observed, especially at the higher substituent concentrations ($y = 0.3$ and 0.4), indicating the presence of mixed phases. The additional peaks in these diffractograms are ascribed to γ-$LiAlO_2$ [27]. It is generally known that replacing the transition metal with Al is not easy because extraneous phases such as Al_2O_3 [29], β-$LiAlO_2$ [30] and γ–$LiAlO_2$ [31], can easily form at calcination temperatures above 600 °C. The lattice parameters for the Fe- and Al-substituted systems, calculated by a least square method, are listed in Table 1. For both the Fe- and

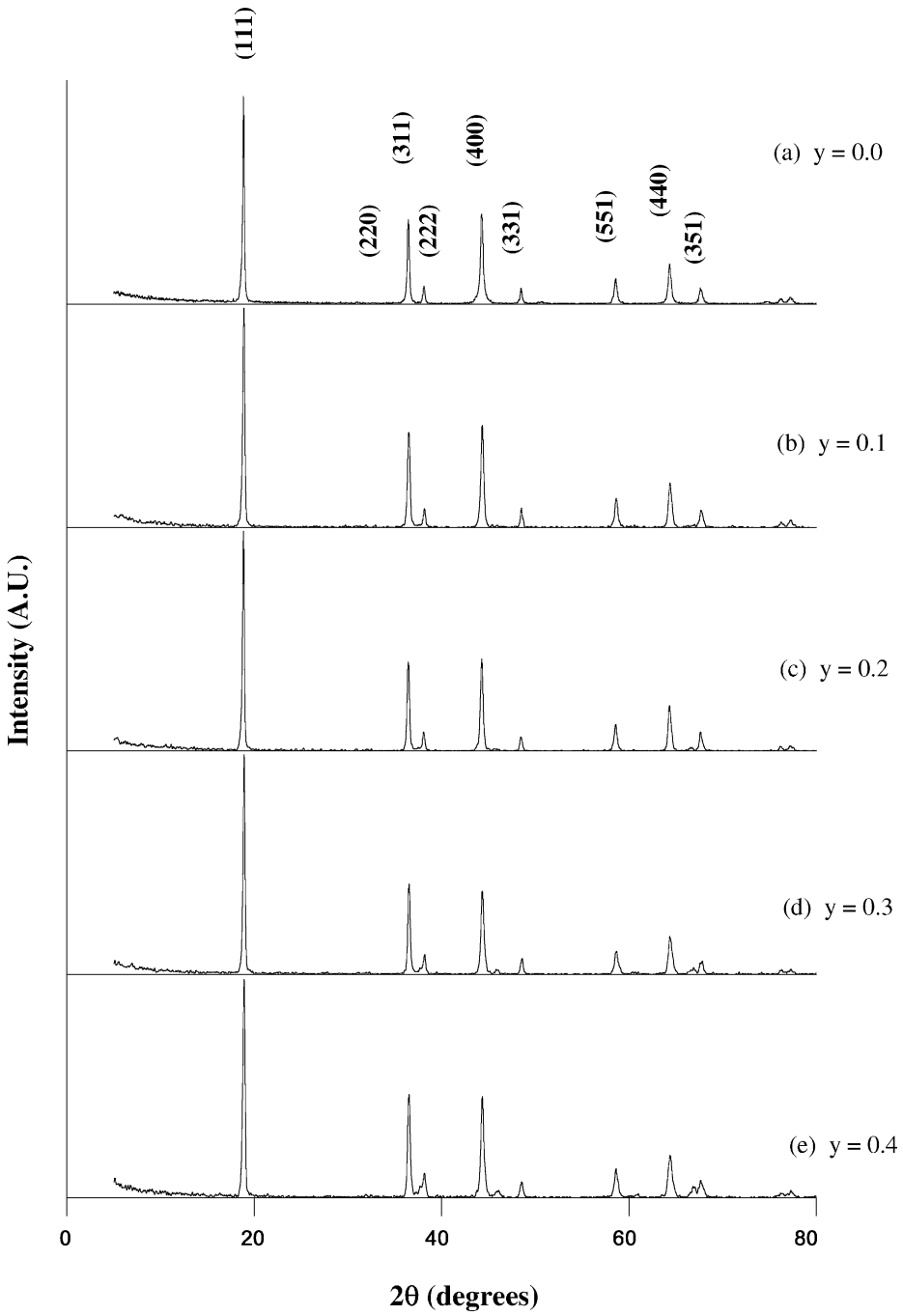

Fig. 2. Powder X-ray diffraction patterns of the $LiAl_yCr_{0.5-y}Mn_{1.5}O_4$ compositions.

Al-substituted systems, the lattice parameter *a* increased linearly with an increase in the substituent content. This is a characteristic feature of solid solutions that obey Vegard's law, according to which some material parameters, such as lattice constants, vary linearly with the mole fraction of the substituent species. The fact that Fe forms complete solid solutions of the general formula $LiFe_yMn_{2-y}O_4$ was demonstrated by Ohzuku et al. [25]. Despite the presence of an extraneous γ-$LiAlO_2$ phase, the linear increase in *a* with Al content is interesting. It must be noted as the Al (or Fe) content (y) was increased, the Cr content ($0.5 - y$) was correspondingly decreased. The decrease in Cr content should have led to an increase in the values of the lattice parameters because in the same oxidation states, chromium ions have smaller ionic radii than manganese ions: Cr^{3+}, 0.615 Å; Mn^{3+}, 0.68 Å; Cr^{4+}, 0.58 Å; and Mn^{4+}, 0.60 Å [32]. Indeed, the values of *a* and the unit cell volume were found to decrease with an increase in the Cr content (Table 1).

An important consideration in substitutional studies is the site occupancy of the substituent ions in the host matrix.

Ohzuku et al. [25] used the integrated intensity ratios of close-lying peaks in the X-ray diffractogram to determine the extent of substituent ion occupancy. In order to ensure desirable electrochemical performance, it is necessary that the substituent ions replace the Mn ions in the 16*d* octahedral sites of the $LiMn_2O_4$ matrix. Any occupancy of the substituent ions in the 8*a* tetrahedral lithium sites will lead to unfavorable electrochemical characteristics. According to Ohzuku et al. [25], the integrated intensity ratios of the (4 0 0)/(3 1 1) and (2 2 0)/(3 1 1) peaks are indices of the extent of substituent ion occupancy in the 8*a* lithium sites. In the case of the $LiFe_yCr_{0.5-y}Mn_{1.5}O_4$ samples, the integrated intensity ratio (4 0 0)/(3 1 1) showed a decrease when the Fe content was increased. However, the (2 2 0)/(3 1 1) increased with an increase in the Fe content. The (2 2 0) peak could be deciphered only at $y = 0.3$ and 0.4. Its intensity increased with the Fe content. Such an increase in the intensity of the (2 2 0) peak and the corresponding increase in the (2 2 0)/(3 1 1) intensity ratio signifies the partial occupancy of the Fe in the lithium 8*a* lattice sites at the higher values of *y*. This was complemented by a decrease in the (4 0 0)/(3 1 1) intensity ratios. However, in the case of the Al-substituted compositions, no peaks corresponding to the (2 2 0) reflections could be seen, but the (4 0 0)/(3 1 1) intensity ratio was found to decrease with an increase in Al content, which suggests that Al showed a propensity to occupy the 8*a* lithium sites in $LiAl_yCr_{0.5-y}Mn_{1.5}O_4$.

3.2. Cyclic voltammetry

The cyclic voltammograms were recorded between 3.00 and 5.10 V. Although electrolyte decomposition was a possibility at the higher voltage, no evidence for any decomposition could be seen in the voltammograms. In fact, $LiPF_6$-based electrolytes, such as the one used in this study, are fairly tolerant to high-voltages [33]. The cyclic voltammograms recorded for the doped systems (Figs. 3 and 4) show two regions of electrochemical activity: one around 4.0 V, corresponding to the lithium intercalation/deintercalation into/from the 8*a* tetrahedral sites and associated with the Mn^{4+}/Mn^{3+} couple, and the other above 4.5 V, corresponding to the oxidation/reduction of the substituent ion. In these samples, besides the common Cr ion, the other substituent ion was either the transition metal ion (Fe) or the non-transition metal ion (Al). Hence, the electrochemical characteristics of the materials must reflect the redox reactions of Mn and Cr, as well as those of the additional substituent species. They must essentially represent any differences between doping with a transition metal cation and doping with a non-transition metal cation.

Fig. 3a and b illustrate the effect of increasing the amount of Fe with a simultaneous decrease in the Cr content. $LiFe_{0.1}Cr_{0.4}Mn_{1.5}O_4$ showed an oxidation peak at 4.15 V corresponding to the oxidation of Mn^{3+} to Mn^{4+}, and a broad peak at 5.04 V with a prominent shoulder at 4.85 V.

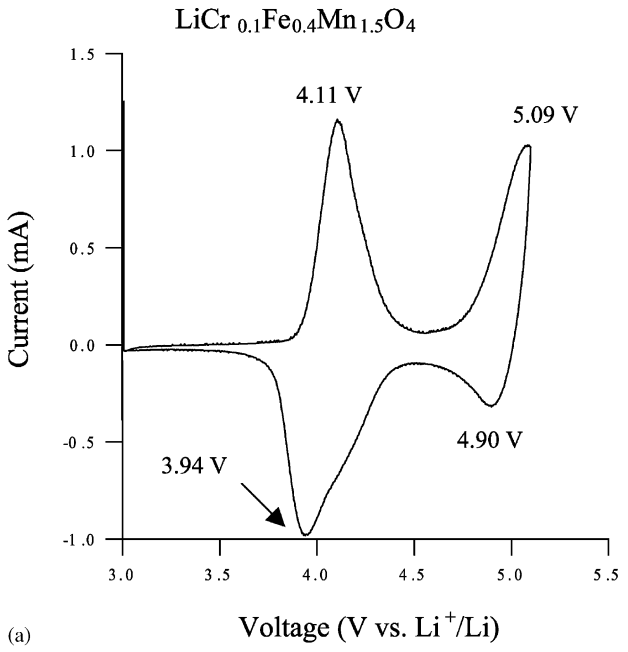

Fig. 3. Cyclic voltammograms of (a) $LiFe_{0.4}Cr_{0.1}Mn_{1.5}O_4$; (b) $LiFe_{0.1}Cr_{0.4}Mn_{1.5}O_4$. Scan rate: 0.1 mV s^{-1}.

While the peak at 5.04 V is attributable to the oxidation of Fe^{3+} to Fe^{4+} [25], the reaction corresponding to the shoulder at 4.85 V is due to the Cr^{4+}/Cr^{3+} couple [8,11,21]. At lower Cr levels, such as in $LiFe_{0.4}Cr_{0.1}Mn_{1.5}O_4$ (Fig. 3a), the shoulder at 4.85 V apparently vanishes, indicating that the contribution from the Cr^{4+}/Cr^{3+} couple is not significant. However, the 5-V peak shifts to 5.09 V. The corresponding reduction peak also shifts from 4.80 to 4.90 V. It is also seen from Fig. 3a and b that an increase in the Fe content from 0.1 to 0.4 resulted not only in a shift of the

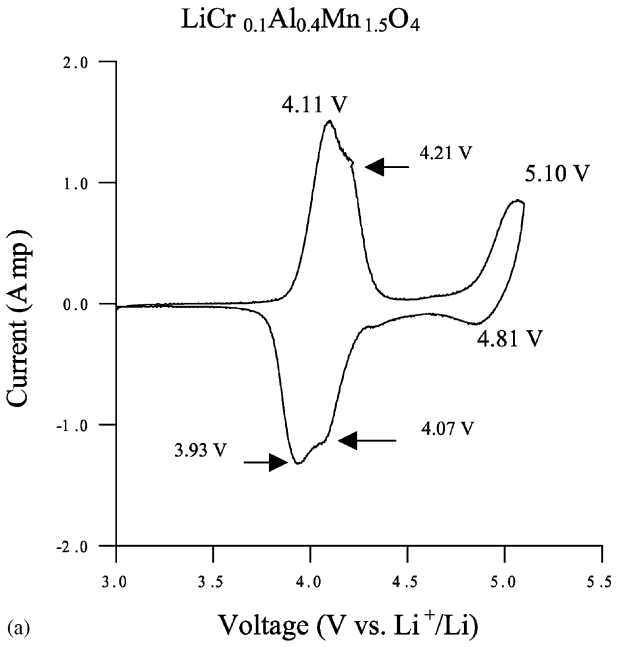

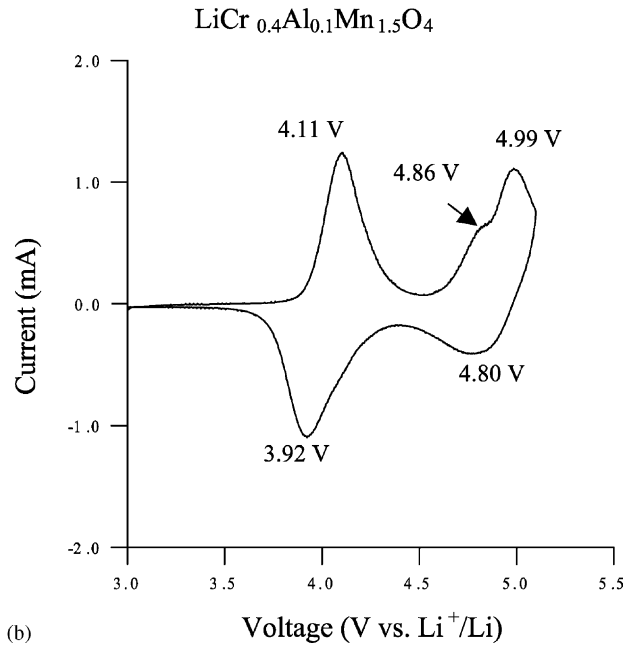

Fig. 4. Cyclic voltammograms of (a) $LiAl_{0.4}Cr_{0.1}Mn_{1.5}O_4$; (b) $LiAl_{0.1}Cr_{0.4}Mn_{1.5}O_4$. Scan rate: 0.1 mV s^{-1}.

redox potential of the Mn^{4+}/Mn^{3+} couple, but also in an increase in the currents associated with the redox peaks. Thus, Fe as a substituent seems to influence the electrochemical characteristics of the Mn^{4+}/Mn^{3+} couple.

However, an examination of the effect of co-substituting with Al (Fig. 4a and b) shows that at high Al-substituent levels, the characteristic pairs of peaks for the Mn^{4+}/Mn^{3+} electrochemical couple [1,34–36] become more prominent, with new shoulders appearing at 4.21 V (oxidation) and at 4.07 V (reduction). Moreover, the shoulder at 4.86 V and the peak at 4.99 V merge into a single peak at 5.10 V as the Al stoichiometry is increased from 0.1 to 0.4. Conversely, the large-area peak at the 5-V region shrinks to a narrow peak as the Cr content is decreased. According to Shao-Horn and Middaugh [37], who investigated the $Li/LiAl_{0.5}Mn_{1.5}O_4$ system, the 5-V oxidation peak has limited reversibility. In fact, the 5-V peak observed with $LiAl_{0.5}Mn_{1.5}O_4$ is totally unexpected given that there is no conventional-type redox couple corresponding to this potential region in $LiAl_{0.5}Mn_{1.5}O_4$. The small reduction current seen around 4.81 V in our samples must have arisen mainly from the conventional reduction reaction of the small amounts of Cr^{4+}. According to Shao-Horn and Middaugh [37], the electrochemical reactions in the 5-V region of substituted $LiMn_2O_4$ spinels may have more to do with the redox reactions of the oxygen lattice, brought about by such substitutions in the spinel framework, than with the conventional redox reactions of the transition metal species. In such a scenario, the split peak around the 5-V region requires further analysis. It is hypothesized that an increase in Mn^{4+} concentration in the spinel due to substitution or extensive lithium de-intercalation is a prerequisite for the occurrence of electrochemical processes around 5-V [37]. For all the compositions, irrespective of whether they had Fe or Al as the co-substituent, the average Mn valency was 3.67. Significantly, there was no shift in the redox peaks corresponding to the Mn^{4+}/Mn^{3+} couple (4.11 V/3.92 V). Thus, co-substitution with Al seems to shift only the oxidation peak of the Cr^{4+}/Cr^{3+} couple to higher potentials. Substitution with non-transition metals has been known to shift the potential of the operating electrochemical couple to higher values. However, Al-substitution does not seem to enhance the currents for the redox processes (Fig. 4a and b). Ceder et al.'s [38] *ab initio* calculations show that the 5-V activity is strongly influenced by the oxygen lattice. However, it looks unlikely that any reversibility in the 5-V region can be attained without a transition metal ion compensating for the charge imbalance created by lithium intercalation/deintercalation.

From the above study, it is clear that the 5-V redox couple is to be attributed to the Cr, and that its potential is tailored by varying the co-substituent concentration. Although tapping the full capacities from these doped materials requires a stable electrolyte, they do represent a class of materials for high energy density lithium batteries.

From the foregoing, it is clear that co-substitution with the cation of a transition metal (Fe) alters the electrochemical behavior of both Mn^{4+}/Mn^{3+} and Cr^{4+}/Cr^{3+} couples. Irrespective of whether it is Fe or Al, the effect is more pronounced in the 5-V region than in the 4-V region. Although Al, as a non-transition metal, is not expected to contribute to capacity through a redox couple, its presence led to a shift in the redox potential of the couple in the 5-V region. The shift increased with an increase in Al content. Thus, although electrochemically inert, non-transition

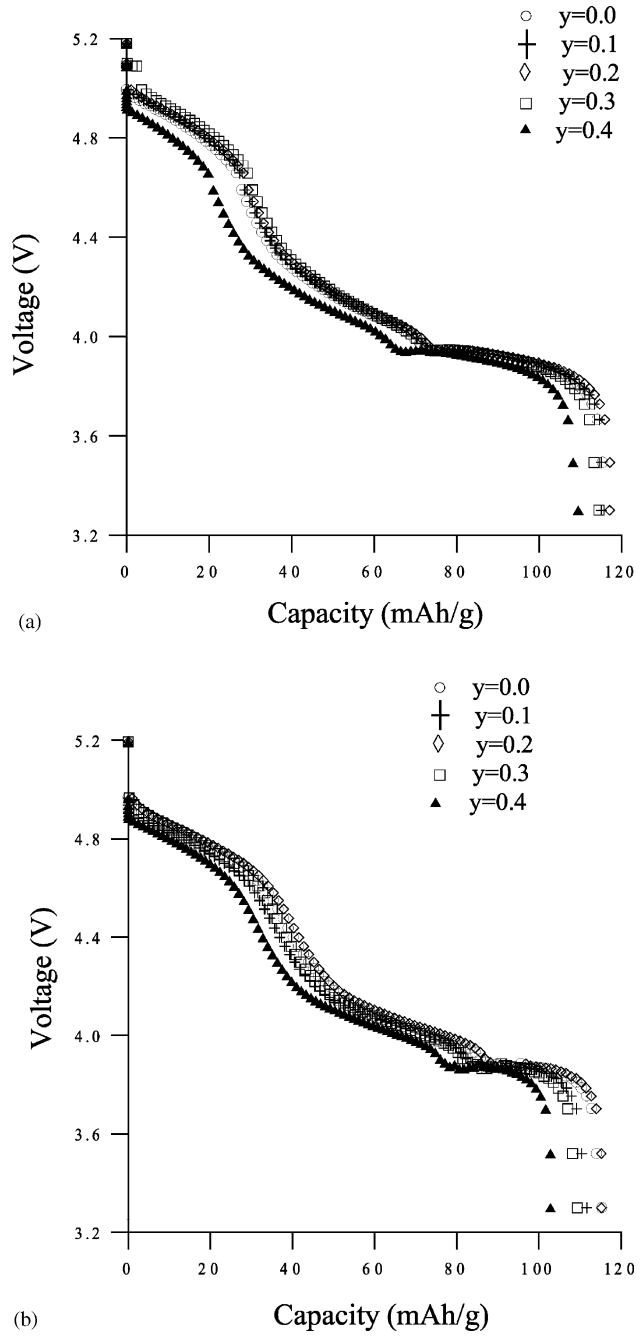

Fig. 5. Typical discharge profiles of $LiM_yCr_{0.5-y}Mn_{1.5}O_4$: (a) M = Fe; (b) M = Al. Charge–discharge rate: 0.1 C.

metal substituent ions can play a role in enhancing the high-voltage capability of the system.

3.3. Charge–discharge studies

Galvanostatic charge–discharge studies were performed between 3.3 and 5.2 V at a 0.1*C* rate. Fig. 5a and b show the two-step discharge profiles of cells with the Fe- and Al-substituted compositions, respectively, reflecting the 4 and 5-V redox processes observed in our cyclic voltammograms. The most striking aspect of the plots is that as the Cr content was increased the capacity in the 5-V region increased. In other words, the capacity in the 4-V region is determined by the Mn^{4+}/Mn^{3+} couple and the capacity in the 5-V region by the Cr^{4+}/Cr^{3+} couple. Similar observations have been reported with Cr-doped $LiMn_2O_4$ [8,11,18,19,21,39]. However, the capacity in the 4-V region was always higher than the corresponding theoretical capacity, and that in the 5-V region was much less than the theoretical value for that region (Table 2: the 4-V capacity is the integral capacity between 3.3 and 4.5 V, whereas the 5-V capacity is that between 4.5 and 5.2 V). The replacement of half the number of trivalent Mn by Cr would mean that the total capacity of the material gets equally shared between the 4 and 5-V regions. Thus, the theoretical 4-V capacity would be 74.7 mAh g^{-1}. Curiously, the observed 4-V capacity was 75.1 mAh g^{-1}, which is higher than the theoretical value. On the other hand, the 5-V capacity was a lower 38.9 mAh g^{-1}. Since the redox potentials of the Mn^{4+}/Mn^{3+} and Cr^{4+}/Cr^{3+} are far apart, at 4.1 and 4.9 V versus Li^+/Li, respectively, an immediate explanation for this abnormal behavior is not forthcoming. Any synergistic effect of the electroactive couples, although it may seem hypothetical at this juncture, should not be discounted. It can also be seen that while the 4-V capacity decreased with an increase in the Cr content, it increased as the Fe content was increased. In the 5-V region, the trend reverses: as the Cr content was increased, the 5-V capacity increased, but decreased as the Fe content was increased. However, the cumulative capacities in all the cases remained in the 103–117 mAh g^{-1} bracket. The two metals seem to have different roles in the two voltage regions studied. Sigala et al. [8,11] and Hong et al. [40] found that Cr as a dopant reduced the 4-V capacity and increased the 5-V capacity. Some authors suggest that the 5-V plateau could be ascribed to the $Mn^{4+} \leftrightarrow Mn^{5+}$ reactions or to the removal of lithium from the octahedral sites in the $LiMn_2O_4$ structure [8,41]. According to Hong et al. [40], the oxidation of Mn^{4+} to Mn^{5+} is a distinct possibility because it involves a change in the electronic configuration from d^3 to d^2, as in the oxidation of Cr^{3+} to Cr^{4+}. Our observations that increased amounts of Fe led to an increase in the 4-V capacity and a reduction in the 5-V capacity run counter to the findings of Song et al. [24] and Ohzuku et al. [39], who investigated $LiFe_yMn_{2-y}O_4$ compositions as cathode materials. Song et al. [24] further reported that as the Fe content increased in $LiFe_yMn_{2-y}O_4$, the intercalation-deintercalation potentials shifted to higher voltage regions. Ohzuku et al. [39], who studied the individual effects of Fe and Cr as substituents in the $LiMn_2O_4$ spinel, found that the charge–discharge profiles of the two doped systems were indistinguishably similar. Obviously, the effect of simultaneous substitution with Fe and Cr differs from the effect of individual substitution.

The occurrence of reversible reactions in the 5-V region for substituted $LiMn_2O_4$ has been attributed solely to the redox behavior of the substituted transition metal ion [8,11,12,21,42–44]. However, if a change in the valence

Table 2
Theoretical and observed first-cycle capacities of the various substituted materials

Composition	4-V capacity (mAh g^{-1})		5-V capacity (mAh g^{-1})		Cumulative capacity (mAh g^{-1})
	Theoretical	Observed	Theoretical	Observed	Observed
$LiMn_2O_4$	148.2	108.0	–	–	108.0
$LiCr_{0.5}Mn_{1.5}O_4$	74.7	75.1	74.7	38.9	114.0
$LiFe_{0.1}Cr_{0.4}Mn_{1.5}O_4$	74.6	81.0	74.6	36.0	117.0
$LiFe_{0.2}Cr_{0.3}Mn_{1.5}O_4$	74.4	83.0	74.4	32.0	115.0
$LiFe_{0.3}Cr_{0.2}Mn_{1.5}O_4$	74.2	83.4	74.2	30.7	114.1
$LiFe_{0.4}Cr_{0.1}Mn_{1.5}O_4$	74.1	85.5	74.1	23.5	109.0
$LiAl_{0.1}Cr_{0.4}Mn_{1.5}O_4$	74.7	77.2	60.6	37.8	115.0
$LiAl_{0.2}Cr_{0.3}Mn_{1.5}O_4$	76.9	86.2	46.1	25.8	112.0
$LiAl_{0.3}Cr_{0.2}Mn_{1.5}O_4$	77.5	87.9	31.0	21.1	109.0
$LiAl_{0.4}Cr_{0.1}Mn_{1.5}O_4$	78.6	88.9	15.7	14.1	103.0

state of a metal ion is an essential criterion for electrochemical activity, no such activity should arise from the Al-substituent. Nevertheless, the Al-substituted spinels exhibited added electrochemical activity. The electrochemical activity due to Al incorporation is akin to that reported with Al-substituted $LiCoO_2$ [45]. *Ab initio* pseudo-potential calculations show substantial charge transfer to the oxygen layer [45,46]. From Table 2, it can be seen that the 4-V capacity of the compounds was always higher than the theoretical values. This suggests a synergistic role for one or more of the substituents in the 4-V activity of the lithium manganese oxide spinel.

For comparison, the cycling performance of the unsubstituted $LiMn_2O_4$ sample was also studied. The charging and discharging in this case were carried out between 3.0 and 4.2 V at a 0.1 C rate. The first discharge capacity of the unsubstituted compound was 108 mAh g^{-1}, while the corresponding value in the 4-V region for the $LiCr_{0.5}Mn_{1.5}O_4$ sample was 75 mAh g^{-1}. The capacity of $LiMn_2O_4$ faded from 108 to 90 mAh g^{-1} in 25 cycles, registering charge retention of 83.3%. Upon substitution with 0.5 atom/molecule of Cr, the cumulative first-cycle capacity was 115 mAh g^{-1}. In the 25th cycle, the capacity was 101 mAh g^{-1} and the capacity retention jumped to 87.8%. Thus, Cr substitution not only increased the capacity, but also resulted in higher charge retention. Fig. 6a and b depict the cycling behavior of cells with the Fe- and Al-substituted $LiM_yCr_{0.5-y}Mn_{1.5}O_4$ compositions. It can be seen from Fig. 6a that when 0.1 atom/molecule of Fe was introduced, the first-cycle capacity rose to 117 mAh g^{-1}. However, an increase in the Fe content from 0.1 to 0.4 in $LiFe_yCr_{0.5-y}Mn_{1.5}O_4$ reduced the first-cycle discharge capacity from 117 to 109 mAh g^{-1}. The corresponding values at the 40th cycle were 88 and 70 mAh g^{-1}, with charge retentions of 75 and 64%, respectively. Thus, as the Fe content was decreased, not only was there a decrease in the deliverable capacity, there was also diminished charge retention. In other words, the replacement of the octahedral site-stabilizing Cr with Fe resulted in decreased stability of the spinel framework. The beneficial effect of Cr in stabilizing the $LiMn_2O_4$ spinel structure has been reported by several groups [8,13–21]. The stronger Cr–O bonds in the delithiated state (compare the binding energy of 1142 kJ mole^{-1} for CrO_2 with 946 kJ mole^{-1} for α–MnO_2 [11]) is a factor in the greater stability of Cr-containing spinels. We have noted earlier that Cr substitution in the $LiMn_2O_4$ spinel reduces unit cell volume, which should increase the stability of the spinel framework during the lithium intercalation/deintercalation processes [11,38,47]. Table 1 shows that as more Cr is replaced with Fe or Al, the unit cell volume increases, contributing to decreased stability for the spinel structure.

Similarly, in the case of $LiAl_yCr_{0.5-y}Mn_{1.5}O_4$, a gradual decrease in the first-cycle capacity was observed as more Cr was substituted with Al. It can be seen from Fig. 6b that as the Al stoichiometry was increased from 0.1 to 0.4, the first-cycle capacity decreased from 112 to 103 mAh g^{-1}. However, these values were lower than the corresponding values obtained with Fe as a co-substituent. Obviously, Fe being a transition metal lends itself to oxidation-reduction reactions, accounting for part of the capacity. The discharge capacities recorded in the 40th cycle with $LiAl_yCr_{0.5-y}Mn_{1.5}O_4$ were 82 and 67 mAh g^{-1} for $y = 0.1$ and 0.4, respectively. The corresponding values for charge retention were 73 and 66%. Al-substitution in the 16*d* octahedral sites of $LiMn_2O_4$ has been shown to bestow relatively good cycling performance [48–50], but our results with simultaneous substitution of $LiMn_2O_4$ with Cr and Al show that an increase in Al content reduces both discharge capacity and cycling stability.

The first-cycle irreversible capacity for $LiMn_2O_4$ was just 9 mAh g^{-1} and for $LiCr_{0.5}Mn_{1.5}O_4$ it was slightly higher at 11 mAh g^{-1}. The irreversible capacity values were considerably higher for the Fe and Al-doped samples. For example, they rose to 40 and 37 mAh g^{-1} for $LiFe_{0.1}Cr_{0.4}Mn_{1.5}O_4$ and $LiAl_{0.1}Cr_{0.4}Mn_{1.5}O_4$, respectively. However, the irreversible capacity values were generally found to decrease with the incorporation of more Fe or Al. The role of the substituent in the irreversible capacity is not immediately clear. In conclusion, despite the fact that the reversible capacities in the 4-V region for the doped compositions were lower

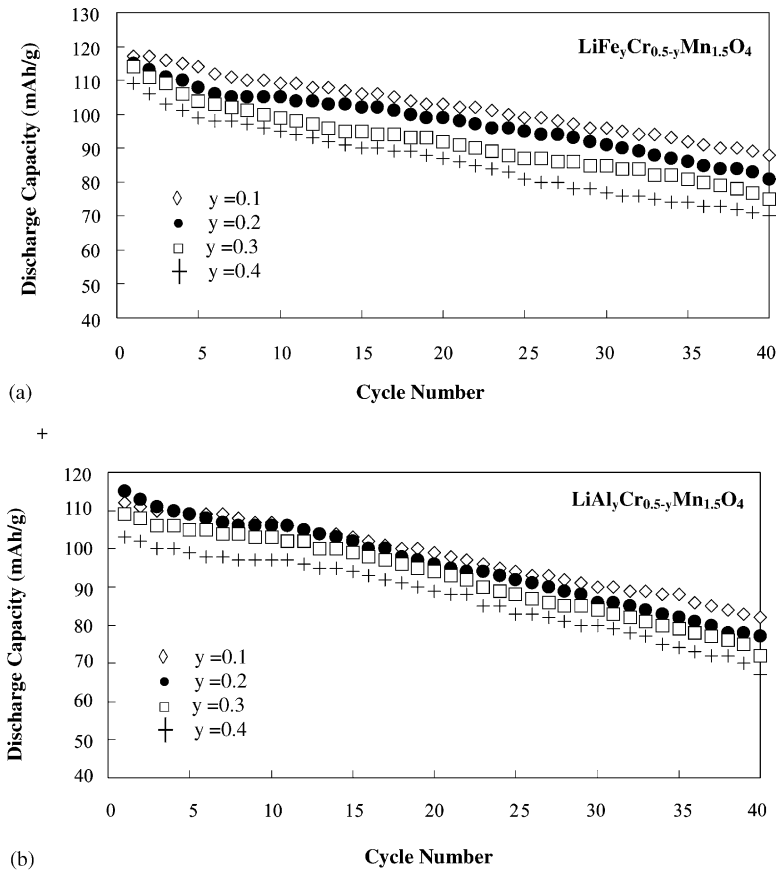

Fig. 6. Cycling performance of $LiM_yCr_{0.5-y}Mn_{1.5}O_4$: (a) M = Fe; (b) M = Al. Charge–discharge rate: 0.1 C.

than that for the undoped $LiMn_2O_4$ (Table 2), the loss in capacity in the 4-V region is more than made up in the 5-V region. Therefore, the cumulative capacity was higher than the capacity of undoped compound. Additionally, the capacities around the higher voltage region represent the higher specific energy of the spinel materials.

4. Conclusions

Simultaneous substitution of Cr and Fe, or Cr and Al for Mn in the $LiMn_2O_4$ spinel was attempted with the aim of developing stable, high-voltage cathode materials of the general formula $LiM_yCr_{0.5-y}Mn_{1.5}O_4$ (M = Fe or Al; y = 0.1, 0.2, 0.3 and 0.4) for lithium-ion batteries. X-ray diffraction studies showed that Fe formed phase-pure compounds in the compositional range studied. However, at Al stoichiometries of 0.3 and 0.4 the Al-substituted materials had γ–$LiAlO_2$ as an impure phase. Both Fe and Al led to an increase in the lattice parameters. It was surmised that as their concentrations increased, the 8*a* tetrahedral propensity of Fe and Al increased. Cyclic voltammograms showed two regions of electrochemical activity: one around 4-V and the other around 5-V, the former associated with the Mn^{4+}/Mn^{3+} couple and the latter with the substituents. Fe as a co-substitutent increased the currents associated with the high-voltage peaks. Fe also influenced the electrochemical behavior of the Mn^{4+}/Mn^{3+} couple. Although Al, as a non-transition metal cannot be expected to enter into redox processes, it gave rise to a peak in the 5-V region, which is attributed to the higher average oxidation state of Mn in the spinel due to doping. Al also enhanced the high-voltage capability of the spinel. Irrespective of whether the co-substituent was a transition metal ion or a non-transition metal ion, it altered the electrochemical characteristics of both the Mn^{4+}/Mn^{3+} and the Cr^{4+}/Cr^{3+} couples. However, the effect was more pronounced in the 5-V region. Although increased amounts of Fe or Al rendered the spinels high-voltage active, both the deliverable capacity and capacity retention were lowered. The cumulative capacities obtainable with Al-substituted materials were less than those with Fe-substituted materials.

Acknowledgements

Financial support by the National Science Council of the Republic of China under contract NSC-90-2214-E-008-003 is gratefully acknowledged. TPK thanks the National Science Council for the award of a post-doctoral fellowship.

References

[1] M.M. Thackeray, W.I.F. David, P.G. Bruce, J.B. Goodenough, Mater. Res. Bull. 18 (1983) 461.
[2] M.M. Thackeray, Prog. Solid-State Chem. 25 (1997) 1.
[3] M.M. Thackeray, J. Electrochem. Soc. 142 (1995) 2558.
[4] Y.K. Sun, Electrochem. Commun. 2 (2000) 6.
[5] Y. Xia, Y. Zhou, M. Yoshio, J. Electrochem. Soc. 144 (1997) 2593.
[6] R.J. Gummow, A. de Kock, M.M. Thackeray, Solid State Ionics 69 (1994) 59.
[7] G.G. Amatucci, C.N. Shmutz, C.N. Blyr, C. Sigala, A.S. Gozdz, D. Larcher, J.M. Tarascon, J. Power Sources 69 (1997) 11.
[8] C. Sigala, A. Verbaere, J.L. Mansot, D. Guyomard, Y. Piffard, M. Tournoux, J. Solid-State Chem. 132 (1997) 372.
[9] M.E. Spahr, P. Novak, O. Haas, R. Nespar, J. Power Sources 68 (1997) 629.
[10] Y.E. Eli, W.F. Howard, S.H. Lu, S. Mukerjee, M. McBreen, J.T. Vaughey, M.M. Thackeray, J. Electrochem. Soc. 145 (1998) 1238.
[11] C. Sigala, D. Guyomard, A. Verbaere, Y. Piffard, M. Tournoux, Solid State Ionics 81 (1995) 167.
[12] Q. Zhong, A. Bonakdarpour, M. Zhong, Y. Gao, J.R. Dahn, J. Electrochem. Soc. 144 (1997) 205.
[13] I.J. Davidson, R.S. McMillan, J.J. Murray, J. Power Sources 54 (1995) 205.
[14] K. Amine, H. Tukamoto, H. Yasuda, Y. Fujita, J. Power Sources 68 (1997) 604.
[15] J.R. Dahn, T. Zheng, C.L. Thomas, J. Electrochem. Soc. 145 (1998) 851.
[16] L. Hernan, J. Morales, L. Sanchez, J. Santos, Solid State Ionics 118 (1999) 179.
[17] S.J. Hong, S.H. Chang, C.H. Yo, Bull. Korean Chem. Soc. 20 (1999) 53.
[18] C. Sigala, A.G. Salle, Y. Piffard, D. Guyomard, J. Electrochem. Soc. 148 (2001) A819.
[19] C. Sigala, A.G. Salle, Y. Piffard, D. Guyomard, J. Electrochem. Soc. 148 (2001) A826.
[20] R. Thirunakaran, B. Ramesh Babu, N. Kalaiselvi, P. Periasamy, T. Prem Kumar, N.G. Renganathan, M. Raghavan, N. Muniyandi, Bull. Mater. Sci. 24 (2001) 51.
[21] H. Kawai, M. Nagata, H. Tukamoto, A.R. West, J. Power Sources 81–82 (1999) 67.
[22] A.F. Wells, Structural Inorganic Chemistry, 3rd ed., Clarendon Press, Oxford, 1962, p. 489.
[23] J. Morales, L. Sanchez, J.L. Tirado, J. Solid-State Electrochem. 2 (1998) 420.
[24] M.Y. Song, D.S. Ahn, S.G. Kang, S.H. Chang, Solid State Ionics 111 (1998) 237.
[25] T. Ohzuku, K. Ariyoshi, S. Takeda, Y. Sakai, Electrochim. Acta 46 (2001) 2327.
[26] J.H. Lee, J.K. Hong, D.H. Jang, Y.K. Sun, S.M. Oh, J. Power Sources 89 (2000) 7.
[27] S.T. Myung, S. Komaba, N. Kumagai, J. Electrochem. Soc. 148 (2001) A482.
[28] Y.S. Lee, M. Yoshio, Electrochem. Solid-State Lett. 4 (2001) A85.
[29] T. Ohzuku, A. Ueda, M. Kouguchi, J. Electrochem. Soc. 142 (1995) 4033.
[30] Q. Zhong, U. von Sacken, J. Power Sources 54 (1995) 221.
[31] Y.I. Jang, B. Huang, H. Wang, D.R. Sadoway, G. Ceder, Y.M. Chiang, H. Liu, H. Tamura, J. Electrochem. Soc. 146 (1999) 862.
[32] W. Borchardt-Ott, Crystallography Springer, New York, 1993.
[33] C. Sigala, A.G. La Salle, Y. Piffard, D. Guyomard, J. Electrochem. Soc. 148 (2001) A812.
[34] M.M. Thackeray, P.J. Johnson, L.A. de Picciotto, P.G. Bruce, J.B. Goodenough, Mater. Res. Bull. 19 (1984) 179.
[35] T. Ohzuku, M. Kitagawa, H. Hirai, J. Electrochem. Soc. 137 (1990) 769.
[36] J.M. Tarascon, E. Wang, F.K. Shokoohi, W.R. McKinnon, S. Colson, J. Electrochem. Soc. 138 (1991) 2859.
[37] Y. Shao-Horn, R.L. Middaugh, Solid State Ionics 139 (2001) 13.
[38] L. Guohua, H. Ikuta, T. Uchida, M. Wakihara, J. Electrochem. Soc. 143 (1996) 178.
[39] T. Ohzuku, S. Takeda, M. Iwanaga, J. Power Sources 81–82 (1999) 90.
[40] S.J. Hong, S.H. Chang, C.H. Yo, Bull. Korean Chem. Soc. 20 (1999) 53.
[41] J.B. Bates, D. Lubben, N.J. Dudney, F.X. Hart, J. Electrochem. Soc. 142 (1995) L149.
[42] H. Kawai, J. Mater. Chem. 8 (1998) 837.
[43] H. Kawai, Electrochem. Solid-State Lett. 1 (1998) 21.
[44] H. Kawai, Chem. Mater. 10 (1998) 3266.
[45] G. Ceder, Y.M. Chiang, D.R. Sadoway, M.K. Aydinol, Y.I. Jang, B. Huang, Nature 392 (1998) 694.
[46] M.K. Aydinol, A.F. Kohan, G. Ceder, K. Cho, J. Joannopoulos, Phys. Rev. B 56 (1997) 1354.
[47] P. Arora, B.N. Popov, R.E. White, J. Electrochem. Soc. 145 (1998) 807.
[48] P. Strobel, M. Anne, Y. Chabre, M.R. Palacin, L. Seauin, G. Vaughan, G.G. Amatucci, J.M. Tarascon, J. Power Sources 81–82 (1999) 458.
[49] D. Song, H. Ikuta, T. Uchida, M. Wakihara, Solid State Ionics 117 (1999) 151.
[50] S.H. Park, K.S. Park, Y.K. Sun, K.S. Nahm, J. Electrochem. Soc. 147 (2000) 2116.